

Research Paper

Swainsonine Activates Mitochondria-mediated Apoptotic Pathway in Human Lung Cancer A549 Cells and Retards the Growth of Lung Cancer Xenografts

Zhaocai Li[#], Xingang Xu[#], Yong Huang, Li Ding, Zhisheng Wang, Gaoshui Yu, Dan Xu, Wei Li, Dewen Tong[✉]

College of Veterinary Medicine, Northwest A&F University, Yangling, Shaanxi 712100, P.R. China

[#] These authors contributed equally to this work.

✉ Corresponding author: Tel: 0086-29-8709-1622. Fax: 0086-29-8709-1032. E-mail: dwtong@nwsuaf.edu.cn.

© Ivyspring International Publisher. This is an open-access article distributed under the terms of the Creative Commons License (<http://creativecommons.org/licenses/by-nc-nd/3.0/>). Reproduction is permitted for personal, noncommercial use, provided that the article is in whole, unmodified, and properly cited.

Received: 2011.11.29; Accepted: 2012.02.19; Published: 2012.02.24

Abstract

Swainsonine (1, 2, 8-trihydroxyindolizidine, SW), a natural alkaloid, has been reported to exhibit anti-cancer activity on several mouse models of human cancer and human cancers *in vivo*. However, the mechanisms of SW-mediated tumor regression are not clear. In this study, we investigated the effects of SW on several human lung cancer cell lines *in vitro*. The results showed that SW significantly inhibited these cells growth through induction of apoptosis in different extent *in vitro*. Further studies showed that SW treatment up-regulated Bax, down-regulated Bcl-2 expression, promoted Bax translocation to mitochondria, activated mitochondria-mediated apoptotic pathway, which in turn caused the release of cytochrome c, the activation of caspase-9 and caspase-3, and the cleavage of poly (ADP-ribose) polymerase (PARP), resulting in A549 cell apoptosis. However, the expression of Fas, Fas ligand (FasL) or caspase-8 activity did not appear significant changes in the process of SW-induced apoptosis. Moreover, SW treatment inhibited Bcl-2 expression, promoted Bax translocation, cytochrome c release and caspase-3 activity in xenograft tumor cells, resulting in a significant decrease of tumor volume and tumor weight in the SW-treated xenograft mice groups in comparison to the control group. Taken together, this study demonstrated for the first time that SW inhibited A549 cancer cells growth through a mitochondria-mediated, caspase-dependent apoptotic pathway *in vitro* and *in vivo*.

Key words: swainsonine, apoptosis, caspase, mitochondrial pathway, A549 cells

Introduction

Swainsonine (1, 2, 8-trihydroxyindolizidine, SW), a natural plant alkaloid, was first isolated from the Australian legume *Swainsona canescens* and then identified in many *Astragalus* and *Oxytropis* species (Leguminosae) [1, 2]. These plants are commonly called locoweeds, found in China, the United States, and some other parts of the world [2, 3]. In China, there are at least 10 species of locoweeds widely growing in the western rangelands covering up to 11 million

hectares [4, 5], which will provide plentiful resources for SW study and application in different field.

SW has attracted great interest for its anti-tumor property. SW not only suppresses the growth and metastasis of murine B16F10 melanoma and MDAY-D2 lymphoid tumor cells in syngeneic mice, but also reduces the growth rate of human melanoma, colon and gastric carcinoma cells, as well as C6 glioma cells *in vitro* and *in vivo* [6-11]. Clinical trials with SW,

as an anti-tumor drug, have shown obviously curative effects with well tolerance in the patients with advanced malignancies [12, 13]. SW has also been shown to promote anti-tumor immunomodulatory activities of immune system and protect both murine and human bone marrow against the toxicity of chemotherapeutic drugs [14-16]. Additionally, the enhancement effects of SW for the performance of anti-tumor agents such as 5-Fu and cisplatin have also reported [17, 18]. All of these studies provide rational for exploring SW as an anti-tumor agent.

Apoptosis is a tightly controlled physiological process that plays a critical role in developmental modeling, homeostasis maintenance, immune repertoires, and clearance of infected or transformed cells [19]. Apoptosis can be triggered by various extracellular and intracellular stimuli via either an extrinsic or intrinsic pathway in different cells [20]. The extrinsic pathway is initiated by cell surface receptors, while the intrinsic pathway is initiated by a mitochondria mediated death signaling cascade [20]. Compared with nontransformed cells, tumor cells are insensitive to some physiological stimuli that trigger physiological cell death. For most of chemotherapy drugs, activation of apoptotic pathways to kill tumor cells is a predominant anti-tumor mechanism. Previous studies showed that SW inhibited the growth of human gastric carcinoma SGC-7901 cells and rat C6 glioma cells via induction of apoptosis [9, 10], suggesting that SW might serve as an apoptotic inducer in tumor cells. Up to date, however, the molecular mechanisms have not yet been investigated. Therefore, we conducted this study to examine the effects of SW on human lung cancer A549 cells both *in vivo* and *in vitro*, and elucidate the possible mechanism involved in this process.

Materials and methods

Reagents

SW was isolated from *Oxytropis kansuensis* Bunge (a kind of locoweed widely distributed in the west of China) and identified by interpretation of spectral data (MS, ¹H NMR, ¹³C NMR, 2D NMR) as described previously [5]. Its purity was evaluated to be above 99%. The alkaloid was dissolved in Ca²⁺- and Mg²⁺-free PBS (0.01 M, pH7.2), at 10 mM as stock solution, sterilized by ultrafiltration, and stored at -20 °C.

RPMI-1640 medium and newborn bovine serum was obtained from GIBCO BRL (Grand Island, NY, US). 3-(4,5-Dimethylthiazol-2-yl)-2,5-diphenyltetrazolium bromide (MTT), 4',6-diamidino-2-phenylindole (DAPI), acridine orange (AO), ethidium bromide (EB), z-VAD-fmk, z-DEVD-fmk, z-LEHD-fmk and z-IETD-fmk were all purchased from Sigma-Aldrich (St. Louis, MO, US). Mouse monoclonal antibodies

against caspase-8, caspase-9, caspase-3, Bcl-2, Bax, Fas, Fas ligand (FasL), cytochrome c, cytochrome c oxidase subunit IV (COX IV), poly (ADP-ribose) polymerase (PARP) and β -actin were purchased from Santa Cruz Biotechnology, Inc. (Santa Cruz, CA, US). Horseradish peroxidase-conjugated secondary antibody was purchased from Wuhan Boster Bio-Engineering Co., Ltd. (Wuhan, China). All other chemicals and reagents were of the highest quality and obtained from standard commercial sources.

Cells culture and treatment

Human lung cancer cell lines A549, Calu-3, SPC-A-1 and H1299 were obtained from the Cell Bank of Type Culture Collection of Chinese Academy of Sciences (Shanghai, China) and cultured in RPMI-1640 medium (GIBCO BRL) supplemented with 10% new born bovine serum (GIBCO BRL), 100 U/ml penicillin and 100 μ g/ml streptomycin, at 37 °C in a 5% CO₂ atmosphere incubator. Cells were treated with SW from a prepared stock solution in PBS, added to the culture medium to obtain final concentrations indicated as in each experiment. Equivalent volume of PBS was used as vehicle.

Cell viability assay

The effects of SW on cell viability were determined using the MTT assay. Briefly, 1 \times 10⁴ cells per well were plated in 96-well culture plates. After overnight incubation, the cells were treated with different concentrations of SW (0, 1.5, 3, 6, 12 or 24 μ M) for 24 h. The cells were treated with 50 μ l of 5 mg/ml MTT and the resulting formazan crystals were dissolved in dimethyl sulfoxide (DMSO). The absorbance was measured by microplate spectrophotometer (Bio-tek Instruments, Inc., Winooski, US) at 570 nm. Results were expressed as percentage of the controls, which were arbitrarily assigned 100% viability.

Apoptosis assessment by DAPI and AO/EB staining

Cells in exponential growth were seeded into 24-well culture plates. After overnight incubation, the cells were exposed to SW. For DAPI staining, the treated cells were fixed with 80% ethanol at room temperature for 30 min. The fixative was removed and the cells were washed with PBS for 3 times, and then incubated with DAPI (1 μ g/ml) for 45 min at room temperature in the dark. For AO/EB staining, the cells without fixation were loaded with a 100 μ l fresh-prepared AO/EB staining solution (100 μ g/ml), then immediately observed under a Nikon fluorescence microscope (Nikon Inc., Japan) in less than 20 min.

Observation of ultrastructural morphology

Transmission electron microscope: After SW treatment, the cells were fixed with 4% glutaraldehyde, and postfixed with 1% OsO₄. Then samples were dehydrated in graded ethanol solutions, followed by embedment and section. Ultrathin sections were stained with uranyl acetate and lead citrate, and then observed under a transmission electron microscope (JEM-1230, Tokyo, Japan) at 60 KV.

Scanning electron microscope: Cells were seeded on cover slips and treated with 12 μM of SW for 24 h, and then washed and fixed in 2.5% glutaraldehyde in PBS for 30 min followed by dehydration in a series of ethanol solutions of decreasing dilution. After critical point dryer and ion sputter were performed, cells were observed under a scanning electron microscope (JSM-6360LV, Tokyo, Japan).

DNA fragmentation assay

After experimental treatment, both adherent and floating cells were collected and washed with PBS. Pellets were then lysed with DNA lysis buffer (20 mM EDTA, 100 mM Tris, pH 8.0, 0.8% SDS) at room temperature for 20 min. After centrifugation for 5 min at 12 000 × g, the supernatants were collected and treated with RNase A (final concentration, 500 μg/ml) for 30 min at 37 °C, followed by digestion with proteinase K (final concentration 500 μg/ml) for 2 h at 55 °C. The DNA was extracted using the phenol / chloroform / isoamylol (25:24:1), precipitated with ethanol, dissolved in TE buffer (10 mM Tris, pH 8.0, 1 mM EDTA), and subjected to 2% agarose gel electrophoresis for DNA fragmentation analysis.

Flow cytometry analysis

Annexin V-FITC / PI apoptosis detection kit (Becton-Dickinson, US) was used for apoptosis detection according to the manufacturer's protocol. Cells were washed twice with PBS and resuspended in 100 μl 1 × Annexin V binding buffer containing 5 μl of Annexin V-FITC and 5 μl of PI. After incubation in the dark for 10 min at room temperature, cells were diluted with 400 μl 1 × Annexin V binding buffer and analyzed by flow cytometry (Beckman Coulter, Inc. Fullerton, CA, US).

Caspase activity assay

Caspases activities were measured by colorimetric assay kits (BioVision, Inc., Mountain View, CA, US) according to the manufacture's recommendations. Briefly, cells were pelleted and lysed on ice, protein concentration was measured using BCA Protein Assay Reagent (Pierce, Rockford, IL, US), then 200 μg of protein was incubated with each caspase

substrate at 37 °C in a microplate for 4 h. Samples were read at 405 nm in microplate spectrophotometer (BioTek Instruments, Inc., Winooski, US).

Western blot analysis

The SW-treated cells were collected and washed with ice-cold PBS, then treated with ice-cold RIPA lysis buffer (Beyotime Inst. Biotech, Beijing, China) with 1 mM phenylmethyl sulfonyl fluoride (PMSF). Cell lysates were centrifuged at 12 000 × g at 4 °C for 5 min. The proteins of mitochondrial and cytosolic fraction were isolated using the Mitochondria / Cytosol Fractionation Kit (BioVision, Inc., Mountain View, CA, US) according to the manufacturer instructions. The protein concentration was determined using the BCA Protein Assay Kit (Pierce, Rockford, IL, US). Equivalent amounts of proteins samples were uploaded and separated by 12% SDS-PAGE and then electrotransferred to polyvinylidene difluoride (PVDF) membrane (Millipore Corp, Atlanta, GA, US). The membranes were blocked in 5% non-fat dry milk in PBS-T at room temperature for 1 h, and then incubated with indicated primary antibodies over night at 4 °C, followed by horseradish peroxidase-conjugated secondary antibodies at room temperature for 1 h. The signal was detected by enhanced chemiluminescence (ECL) reagents (Pierce, Rockford, IL, US).

Real-time RT-PCR analysis

Total RNA was isolated from SW-treated cells and reverse transcribed with MMLV reverse transcriptase and oligodT primers. Quantitation of genes coding for Bcl-2 was performed using SYBR Premix Ex Taq™ II kit (Takara, Dalian, China) by Bio-Rad iQ 5 Real Time PCR System. The β-actin gene was used as an endogenous control. The primer sequences were: TTGAGGAAGTGAACATTTCCGGTG (forward), AGGTTCTGCGGACTTCGGTC (reverse) for Bcl-2; AGTTGCGTTACACCCITTTCTTG (forward), TCACCTTCACCGTTCAGTTT (reverse) for β-actin. The gene expression fold changes were calculated using cycle time (Ct) values as described previously [21].

Antitumor activity in vivo

Female congenital athymic BALB/c nude (nu/nu) mice were purchased from Shanghai National Center for Laboratory Animals (Shanghai, China) and maintained in pathogen-free conditions. Exponentially growing A549 cells suspended in serum-free medium were injected subcutaneously into the back of the 4-weeks old mice (1×10⁶ cells in 100 μl). After tumor transplantation for 1 week, mice were divided randomly into three groups (n = 6) and orally

administrated PBS (control group), 1 mg/kg/d or 2.5 mg/kg/d doses of SW in PBS in a 0.2-ml volume, respectively, for 15 consecutive days. These doses are chosen as safe and effective in mice model according to the previous report [8]. The length (a) and width (b) of tumor were regularly measured for 3-4 times every week by a caliper and the tumor volumes were then calculated according to the formula $[(a \times b^2) / 2]$. At the termination of the experiment, xenograft tumors were excised and weighed to record wet tumor weight. A portion of the tumors from control and treated animals were fixed in 4% paraformaldehyde, embedded in paraffin, and cut into 6 μm sections for histologic study, and that the rest were used for preparation of tumor lysate used in further experiments. The animal experiments were performed in accordance with the 'Guidelines for Animal Experimentation' of the Forth Military Medicine University.

TUNEL assay

Xenograft tumors were fixed in 4% paraformaldehyde, embedded in paraffin and cut into 6 μm sections. Terminal deoxynucleotidyl transferase-mediated dUTP nick end labeling (TUNEL) assay was conducted to study DNA fragmentation using the *in situ* cell death detection kit (Beyotime Inst. Biotech, Beijing, China) according to the manufacturer's instructions. After mounting the TUNEL positive cells, the sections were observed at $\times 400$ magnification under a Nikon microscope (Nikon Inc., Japan).

Immunohistochemistry analysis the expression of Bax and Bcl-2

Fresh tumor tissue sections were incubated with primary antibodies against Bax (1:100) and Bcl-2 (1:100) (Santa Cruz Biotechnology, US), biotinylated secondary antibody IgG, respectively, followed visually using SABC kit according to its protocol (Maixin Biological Technology Company, Fuzhou, China). The tissue sections were viewed at $\times 400$ magnification under a Nikon microscope (Nikon Inc., Japan).

Statistical analysis

Data are expressed as the means \pm SD. For each assay, student's *t*-test was used for statistical comparison. A probability of $p < 0.05$ was considered significant.

Results

SW inhibits the growth of various human lung cancer cell lines

Firstly, we investigated the effects of SW treatment on the growth of various lung cancer cell lines,

including A549, Calu-3, H1299 and SPC-A-1. As shown in Fig. 1, SW inhibited the growth of these cell lines in a concentration-dependent manner. 3 μM of SW significantly reduced the cell viabilities of all tested cell lines after 24 h exposure.

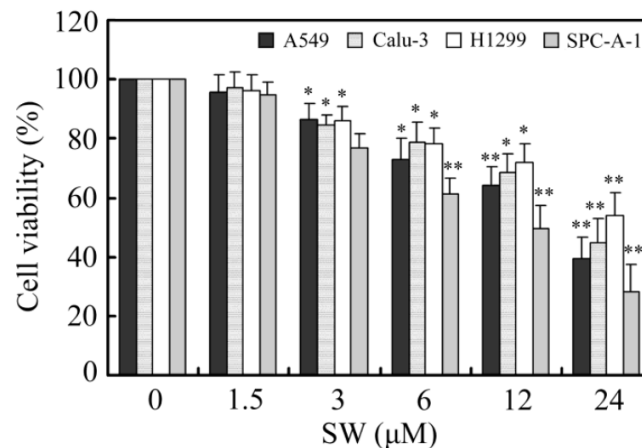


Figure 1. The effects of SW treatment on different lung cancer cell lines. Cells were seeded in 96-well plates and treated with various concentrations of SW for 24 h. After the end of treatment, cell viabilities were determined by MTT assay. The values were calculated relative to the control group (0 μM). The results are mean \pm SD and representative of three independent experiments. * $p < 0.05$; ** $p < 0.01$ versus the control group (0 μM of SW).

SW treatment induces apoptosis in human lung cancer A549 cells

To determine whether the observed decrease in cell viability was associated with apoptosis, we examined the nuclear morphology using a Nikon fluorescence microscope. A549 cells were treated with different concentrations (0, 3, 6, 12 and 24 μM) of SW for 24 h (Fig. 2A, B), or 12 μM of SW for indicated times (Fig. 2C, D), followed by DAPI and AO/EB staining. The control cells did not appear significant changes in cell nuclei and cell membrane integrity, whereas SW-treated cells appeared different extent of chromatin condensation, nuclear fragmentation and destruction of cell membrane integrity after 24 h of incubation with different concentrations of SW, particularly with 24 μM of SW (Fig. 2A, B). Typical apoptotic nuclei were observed as early as 12 h in cells treated with 12 μM of SW (Fig. 2C, D). Characteristically morphological changes of apoptosis were also observed under transmission and scanning electron microscope in A549 cells treated with 12 μM of SW for 24 h, including cell shrinkage, volume reduction, chromatin condensation, cell blebbing and formation of membrane embedded apoptotic bodies (Fig. 2E, F).

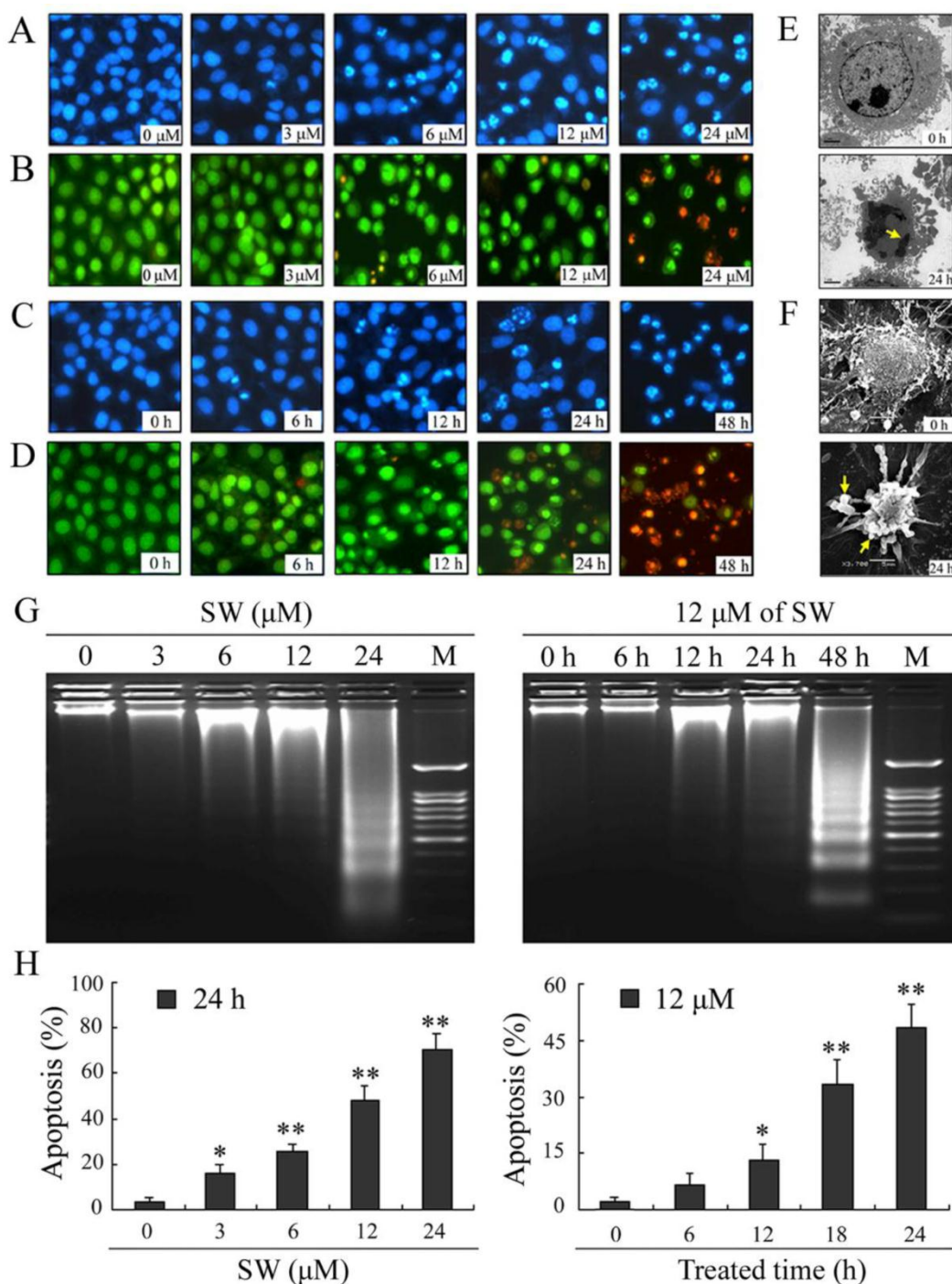


Figure 2. SW induces concentration- and time-dependent apoptosis in A549 cells. (A-D) Cells were treated with SW at different concentrations (0-4 μM) for 24 h (A, B) or treated with 12 μM of SW for different times (0-48 h) (C, D). Nuclear morphological changes in A549 cells were observed under fluorescent microscope after DAPI or AO/EB staining (400 \times). (E, F) Cells were treated with 12 μM of SW for 24 h. Ultrastructural morphology was visualized under transmission electron microscopy (E) and scanning electron microscopy (F). Arrows show chromatin condensation (E) and membrane embedded apoptotic bodies (F). (G) Induction of DNA fragmentation. DNA isolated from SW-treated cells was subjected to 2% agarose gel electrophoresis, followed by visualization of bands and photography. (H) Apoptosis rate of A549 cells. SW-treated cells were stained with Annexin V-FITC and PI for 10 min at room temperature, followed by FCM analysis. The Annexin V positive cells were regarded as apoptotic. The results are mean \pm SD and representative of three independent experiments. * $p < 0.05$, ** $p < 0.01$ versus the control group.

Besides changes in cell morphology, DNA fragmentation of SW-treated cells was also examined by observation of the formation of DNA ladder. As shown in Fig. 2G, DNA ladder appeared to be more evident with the increasing of SW concentration, however, no DNA fragments were observed in the control groups (Fig. 2G, left panel). When the cells were treated with 12 μM of SW, DNA fragments were observed at 12 h, and more evident at 48 h (Fig. 2G, right panel). The SW-induced apoptosis was further determined by flow cytometry using Annexin V/PI dual staining. When A549 cells were treated with different concentrations (0-24 μM) for 24 h, the average percentage of apoptotic cells (Annexin V⁺) increased from 3.2% of the control to 71.5% (Fig. 2H, left panel). When the cells were treated with 12 μM of SW for indicated time (0-24 h), the rate of apoptotic cells significantly increased over 12 h, and reached about 42.7% over 24 h of incubation (Fig. 2H, right panel). Taken together, these results demonstrated that SW treatment induced A549 cells apoptosis in a concentration- and time-dependent manner. In addition, SW-induced apoptosis was also observed in Calu-3 cells, H1299 cells and SPC-A-1 cells (Fig. 3A, B).

Activation of caspase-9 and -3, but not caspase-8, is involved in SW-induced apoptosis

In the present study, we investigated the possible mechanisms of SW-induced apoptosis in A549 cells. Since caspases are known to play a pivotal role in mediating various apoptotic signaling, we measured the activity of initiator caspases (caspase-8 and -9) and effector caspase (caspase-3) in SW treated cells. As shown in Fig. 4A, exposure of A549 cells to 12 μM of SW led to increased levels of activated caspase-9 and -3 and caused cleavage of PARP in a time-dependent manner during the treatment period. The activated forms of caspases-9 and -3 were observed as early as 6 h. In contrast, the cleavage pro-caspase-8 was not observed in this study. The SW-induced caspases activation was further confirmed by measuring the enzymatic activities of caspases-8, -9, and -3 using the colorimetric assay kits. As shown in Fig. 4B, SW-treatment significantly increased the activities of caspases-9 and -3 but had no effects on the activity of caspase-8 during the treated period.

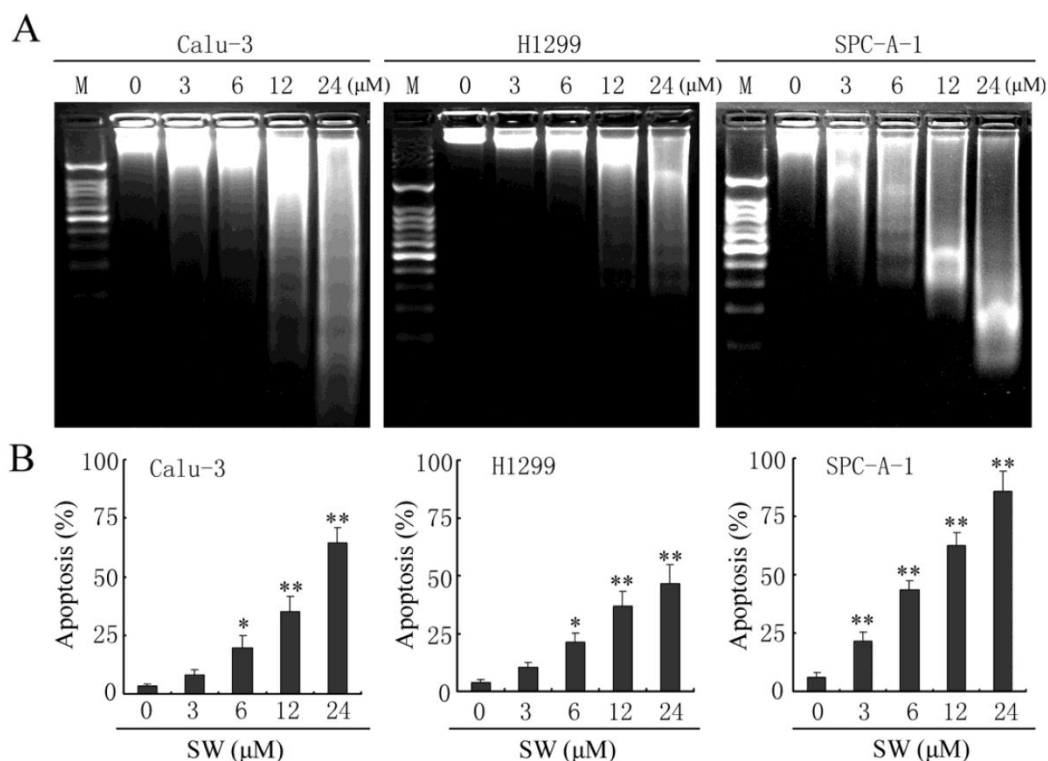


Figure 3. SW induces apoptosis in Calu-3, H1299 and SPC-A-1 cells. (A) Calu-3, H1299 and SPC-A-1 cells were treated with the indicated concentrations of SW for 48 h. DNA was extracted and analyzed on 2% agarose gel. (B) Calu-3, H1299 and SPC-A-1 cells were treated with the indicated concentrations of SW for 24 h, followed by Annexin V / PI staining and FCM analysis. The Annexin V positive cells were regarded as apoptotic. The results are mean \pm SD and representative of three independent experiments. * $p < 0.05$, ** $p < 0.01$ versus the control group (0 μM).

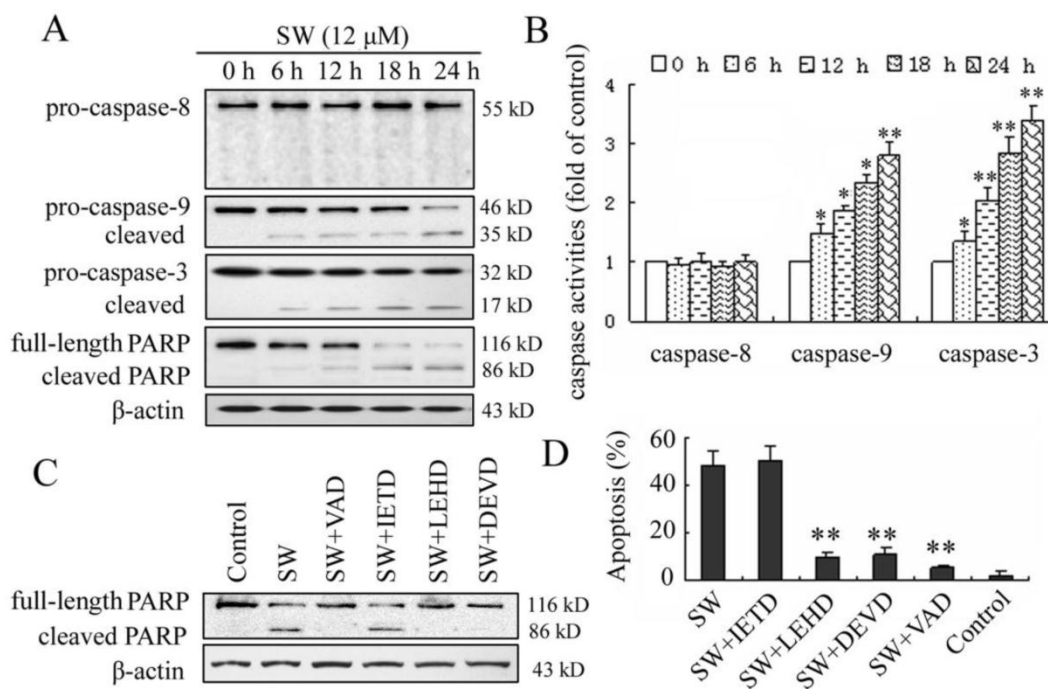


Figure 4. SW-induced apoptosis is mediated by activation of caspase-9 and -3. (A) A549 cells were treated with 12 μ M of SW for indicated time. Whole cell lysates were subjected to western blot analysis to detect total and activated caspase-8, -9, -3 and PARP. The data shown are representative of three independent experiments. (B) Caspase activities in cells treated with SW. Cells were incubated with 12 μ M of SW for indicated times and the enzymatic activities of caspases-8, -9, and -3 were measured using the colorimetric assay kits. The results are mean \pm SD and representative of three independent experiments. * $p < 0.05$, ** $p < 0.01$ versus the control group (0 h). (C) Effect of caspase inhibitors on SW-induced cleavage of PARP. Cells were incubated with 20 μ M of caspase inhibitors, z-VAD-fmk, z-DEVD-fmk, z-IETD-fmk or z-LEHD-fmk for 1 h and then co-incubated with 12 μ M of SW for 24 h. Expression level of PARP was analyzed by Western blot. The data shown are representative of three independent experiments. (D) Effects of caspase inhibitors on SW-induced apoptosis. A549 Cells were treated as in C. Rate of apoptosis was evaluated by FCM analysis. Data are mean \pm SD and representative of three independent experiments. ** $p < 0.01$ versus SW alone without inhibitor.

To further determine the involvement of caspases in SW-induced apoptosis, four caspase inhibitors, z-VAD-fmk (pan caspase inhibitor), z-IETD-fmk (caspase-8 specific inhibitor), z-LEHD-fmk (caspase-9 specific inhibitor) and z-DEVD-fmk (caspase-3 specific inhibitor) were used to block intracellular protease, and then the SW-induced cleavage of PARP and apoptotic rate was detected using western blot and flow cytometry assay. Z-VAD-fmk, z-LEHD-fmk, or z-DEVD-fmk inhibited SW-induced cleavage of PARP, whereas z-IETD-fmk (caspase-8 inhibitor) did not (Fig. 4C). In consistent with this result, the apoptosis of SW-treated cells was prevented almost wholly by z-VAD-fmk, in part by z-LEHD-fmk and z-DEVD-fmk, but not by z-IETD-fmk after 24 h of co-treatment (Fig. 4D). These results suggested that the SW-induced apoptosis was dependent on the activation of caspases and mainly executed through the activation of caspase-9 and -3.

SW treatment activates the mitochondrial apoptotic pathway involving the regulation of Bcl-2 family members

Apoptosis is usually induced through two distinct signaling pathways: the death receptor pathway and the mitochondrial pathway. The death receptor pathway is usually triggered by ligation of death receptors such as Fas or tumor necrosis factor receptor, which recruits fas associated protein with death domain (FADD) and procaspase-8 to form a death-inducing signaling complex, leading to caspase-8 proteolytic activation. Activated caspase-8 can not only directly activates downstream caspase-3, but also cleave Bid to truncated Bid (tBid), which in turn activates the mitochondrial pathway [22]. Consistent with the results of caspase-8, SW treatment also did not affect the levels of Fas and FasL, or promote cleavage of Bid (Fig. 5A, B). These results further suggested that SW treatment might not activate Fas-mediated death receptor pathway in A549 cells.

The mitochondrial pathway usually involves the release of mitochondrial cytochrome c to the cytosol. Once released, cytochrome c combines with apoptotic protease activating factor 1 (Apaf-1) and procaspase-9 to form the apoptosome in the presence of ATP, resulting in the activation of caspase-9 and caspase-3 [23]. The Bcl-2 family members are known to play important roles in controlling the release of cytochrome c from mitochondria. Upon apoptotic signals, pro-apoptotic Bcl-2 members, such as Bax, Bak or Bid, are activated; in contrast anti-apoptotic Bcl-2 member Bcl-2 and Bcl-X_L can prevent this occurrence [24]. The imbalance of expression of pro- and anti-apoptotic proteins is associated with the ultimate fate of cells [25]. To assess whether mitochondrial pathway is involved in SW-induced apoptosis, we evaluated the expression levels of Bax and Bcl-2 by western blot. As shown in Fig. 5B, exposure of A549 cells to 12 μ M of

SW for different times (0-24 h), Bax protein levels increased, whereas Bcl-2 protein levels decreased gradually with time. Thus, SW treatment increased the ratio of Bax/Bcl-2, which is in favor of the occurrence of apoptosis. The reduction of Bcl-2 in mRNA levels might contribute to the shift in the Bax/Bcl-2 ratio (Fig. 5C). Next, we detected the location of Bax and cytochrome c in the proteins extracts from both mitochondrial and cytosolic fractions of SW-treated cells. A translocation of Bax from cytosol to mitochondria was observed as early as 6 h post-treatment (Fig. 5D). Consistent with this, a time-dependent decrease in mitochondrial cytochrome c and a concomitant increase in the cytosolic fraction were also observed (Fig. 5D). These results suggested that SW treatment-induced apoptosis was mainly through the activation of mitochondrial pathway.

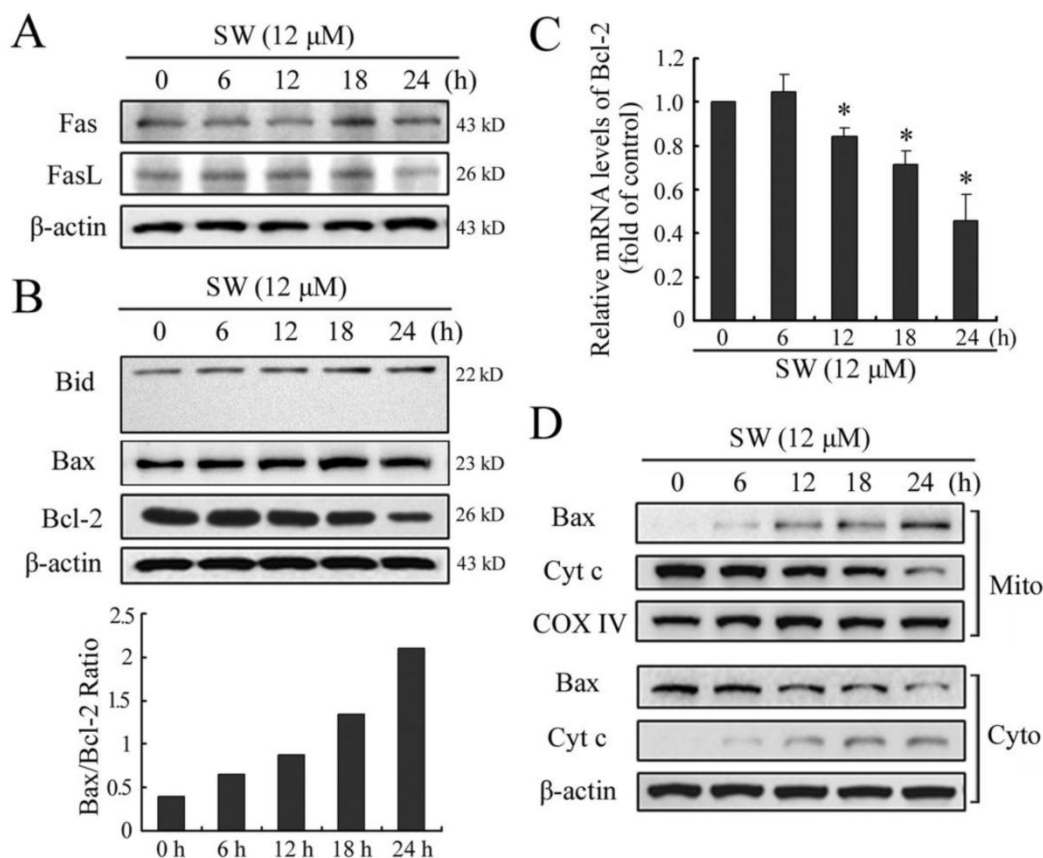


Figure 5. SW-induced A549 cell apoptosis is mediated by the activation of mitochondrial pathway. A549 cells were incubated with 12 μ M of SW for indicated time. The cell lysates were subjected to Western blot analysis, while total RNA was extracted and used for real-time RT-PCR assay. (A) SW treatment did not affect the levels of Fas or FasL. (B) SW treatment did not promote the cleavage of Bid, but increased the ratio of Bax/Bcl-2. The values were calculated from the bands corresponding to Bax and Bcl-2 that normalized to β -actin. (C) SW treatment decreased the expression of Bcl-2 at mRNA levels. The results are mean \pm SD and representative of three independent experiments. * $p < 0.05$ versus the control group (0 h). (D) SW treatment promoted Bax translocation and cytochrome c release. Cells were treated with 12 μ M of SW for the indicated times. The cytosolic and mitochondrial fraction proteins were collected and then detected by western blot. COX IV and β -actin were used as internal controls for the mitochondrial fractions and the cytosolic fraction, respectively. All the data shown are representative of three independent experiments.

SW intake inhibits growth of A549 xenografts in athymic nude mice

SW has been shown to be effectively induced apoptosis in A549 cells; therefore, we further extended our study to determine whether these events occur *in vivo* using a xenograft mouse model. Athymic nude mice xenografted with A549 cells were divided into control group and SW-treated groups wherein SW was administered at doses of 1 or 2.5 mg/kg/day for 15 days. Contrast with control group, tumor volume was inhibited by 27% and 41% ($p < 0.05$) and the wet weight of tumor was decreased by 24% and 36% ($p < 0.05$) in 1 and 2.5 mg/kg/day SW-treated group, respectively, at the termination of the experiment (Fig. 6A, B). SW administration did not seem to induce any adverse effects as judged by monitoring body weight and livers and kidneys (data not shown). No pathological changes were observed in the lung histology of mice from the SW-treated group (Fig. 6C, left panel). Furthermore, we evaluated the effects of SW intake on the induction of apoptosis and apoptosis-associated molecules in tumor xenografts. TUNEL assay showed evident *in situ* apoptosis in A549 tumor sections at 1 and 2.5 mg/kg/day of SW-treated groups, but not in the sections of control group (Fig. 6C mid panel). Immunohistochemistry and western blot analysis showed that SW administration resulted in an increase in the protein levels of Bax, decrease in Bcl-2 and simultaneous activation of caspase-3, the redistribution of Bax and cytochrome c compared to mice receiving vehicle treatment (Fig. 6C right panels, D), which is consistent with our findings in cell culture. These data suggested that SW administration inhibited A549 xenograft tumors growth via induction of tumor cell apoptosis.

Discussion

Previous studies have shown that SW inhibits a number of human tumors including colorectal carcinoma, melanoma, hepatoma, breast carcinoma, pate malignant tumor and gastric carcinoma as well as in murine lymphoma tumor cells, melanoma cell, S180 ascites tumor and rat glioma cells *in vitro* or *in vivo* [8-10, 12, 26]. In the present study, we evaluated the effects of SW on several human lung cancer cell lines *in vitro* and A549 *in vivo*. The results demonstrated that SW reduced the survival of the cancer cells and inhibited the growth of A549 xenograft tumors through induction of apoptosis. In addition, we provided evidence that SW induced apoptosis in A549 cells through the cytochrome c-mediated, caspa-

se-dependent pathway.

Many previous reports have indicated that a lot of anticancer drugs or cancer chemopreventive agents act through the induction of apoptosis to prevent tumor promotion and progression [27, 28]. Sun *et al.* reported that the growth inhibition effect of SW on SGC-7901 cells and C6 glioma cells might be through induction of apoptosis [9, 10]. In the current *in vitro* study, we observed that SW inhibited cell growth through induction of apoptosis in A549 cells in a concentration- and time-dependent manner, as evident by the phosphatidylserine externalization, appearance of membrane enclosed apoptotic bodies, DNA laddering fragment, as well as caspases activation and PARP cleavage. SW has been reported to inhibit solid tumors through direct and indirect actions on the tumor cells *in vivo*, and the two possible mechanisms have been elucidated in previous studies. Firstly, it inhibits tumor cell metastasis and invasion by modifying the expression of glycoprotein on the tumor cell surface as an oligosaccharide-processing inhibitor. Tumor cells cultured in the presence of SW show loss of invasiveness into extracellular matrix, as well as loss of organ colonization potential when injected i.v. into mice [29]. Secondly, SW acts as an anticancer immunomodulatory agent. SW alleviates tumor-induced immune suppression and stimulates NK cell, macrophage, and LAK cell-mediated tumoricidal activity [16, 26, 30, 31]. In this study, significant apoptosis were observed by TUNEL assay in the xenograft tumors in mice orally received SW at doses of 1 and 2.5 mg/kg/day. Our results demonstrate that SW also serves as an apoptosis inducer both *in vitro* and *in vivo*.

Next, we investigated the possible mechanisms of SW-induced apoptosis in A549 cells. Caspases have been known to play a pivotal role in the execution of apoptosis. The two major caspases activation pathways, i.e., death receptor and mitochondrial pathways, have been well described [20]. In death receptor pathway, apoptosis occurs upon the stimulation of death receptors in the cell surface to activate caspase-8. The mitochondrial pathway is dependent on the release of cytochrome c from mitochondria to the cytosol, resulting in the activation of caspase-9. Caspase-8 and caspase-9 will then proteolytically activate downstream caspases, in particular caspases-3, which is essential for the morphological change and DNA fragmentation associated with apoptosis. There are also evidences that apoptosis can be induced through caspase-independent mechanism [32].

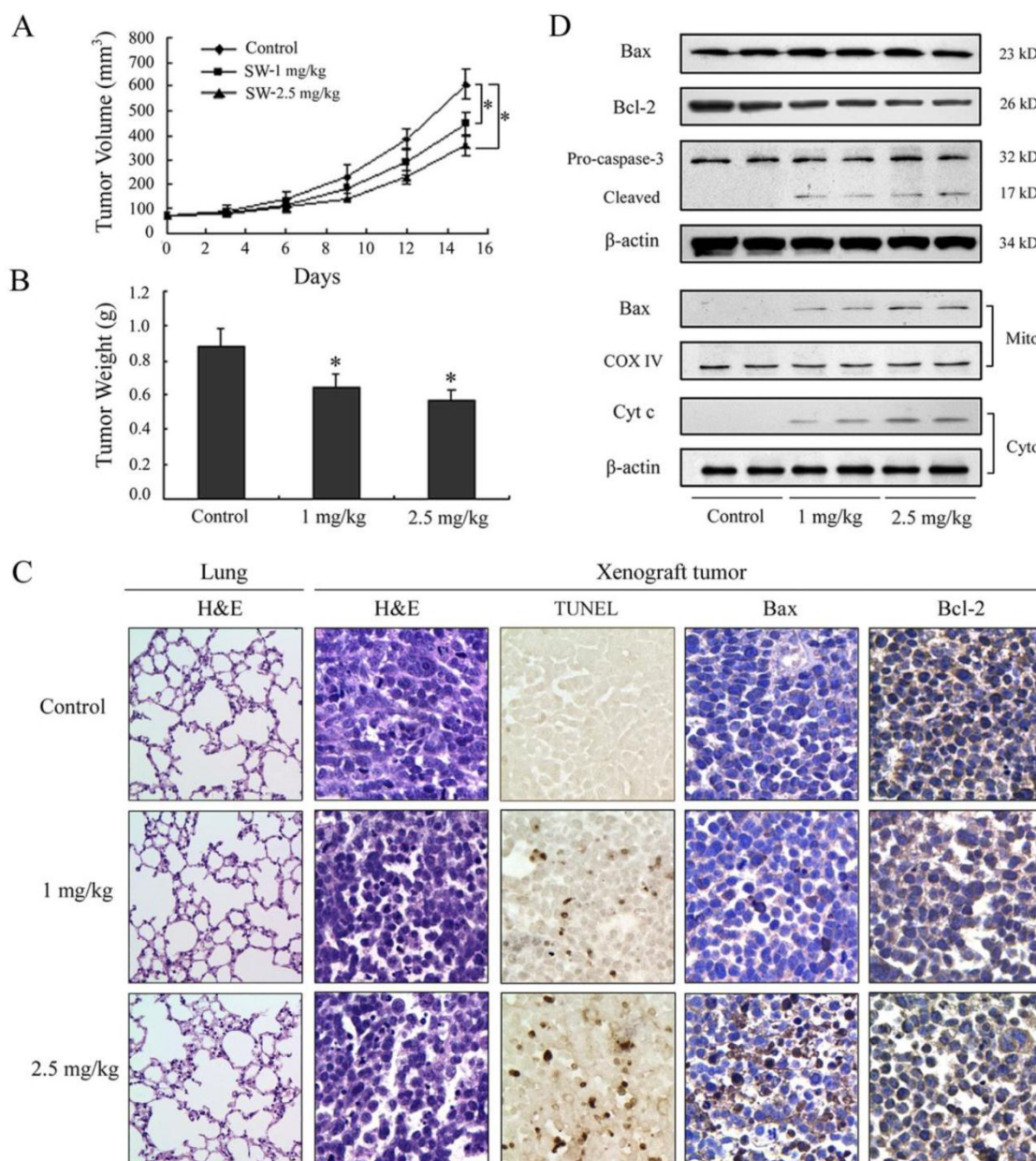


Figure 6. SW administration inhibits A549 tumor growth in athymic nude mice via induction of apoptosis. Approximately 1×10^6 A549 cells were injected into back of mouse, and SW was provided to mice 1 week after cell inoculation. Mice were divided into three groups: Group I received 0.2 ml PBS only as control; Group II received 1 mg/kg SW in 0.2 ml PBS; Group III received 2.5 mg/kg SW in 0.2 ml PBS daily for 15 days. (A) Tumor volumes (mm^3) were measured regularly in two dimensions throughout the study. Data are represented as the mean of 6 tumors from each group. * $p < 0.05$ versus the control group. (B) Wet weight of tumors were measured in the end of this experiment. Data are represented as the mean of 6 tumors from each group. * $p < 0.05$ versus the control group. (C) The host's lung tissues were examined by H&E staining. Tumor tissues were examined by H&E staining, TUNEL assay and immunohistochemistry staining with anti-Bax and Bcl-2 primary antibodies. (D) Western blot analysis of cytochrome c, Bax, Bcl-2, and caspase-3 in tumor tissue lysates after intake of indicated doses of SW. The data are representative of three independent experiments.

In this study, we observed that the process of SW-induced apoptosis involved the activation of caspase-9 and -3, and that the treatment with pan-caspase inhibitor or specific inhibitors of caspase-9 and -3 significantly prevented the SW-induced cell apoptotic effects. Thus, our results demonstrate

that the SW-induced apoptosis is dependent on the activation of caspases, especially caspase-9 and -3. As a low molecular weight and water soluble alkaloid, SW can quickly enter the cytoplasm rather than persistently stay on the cell membrane, which implies the possibility that mitochondria-mediated caspase-9/-3

activation pathway should be responsible for the SW induced apoptosis. Coincidentally, SW treatment did not activate caspase-8 or its upstream molecules such as Fas and FasL. Just like some compounds such as sulforaphane and γ -tocotrienol, which induce apoptosis by directly impairing the mitochondrial integrity in certain cell types [33, 34], SW failed to activate the death receptor-mediated caspase-8 pathway in this study.

Mitochondria play an essential role in death signal transduction and amplification of the apoptotic response. An important role of mitochondria in apoptotic signaling is the translocation of cytochrome c from the mitochondrial intermembrane compartment into the cytosol. Once released, cytochrome c together with Apaf-1 activates caspase-9, and the latter then activates caspase-3 [35]. The release of cytochrome c and cytochrome c-mediated apoptosis is controlled prominently by the members of Bcl-2 family, of which Bax and Bcl-2 have been identified as major regulators. In response to a variety of stimuli including anticancer drugs, Bax translocates to the mitochondria and inserts into the outer mitochondrial membrane, where allows the release of cytochrome c. In contrast, Bcl-2 blocks cytochrome c efflux by binding to the outer mitochondrial membrane and forming a heterodimer with Bax resulting in neutralization of its proapoptotic effects [36]. Therefore, the balance between the levels of Bcl-2 and Bax is critical in determining the fate of cells, survival or death. Results obtained in the present study demonstrated that SW-treatment increased the ratio of Bax/Bcl-2, promoted the redistribution of Bax and cytochrome c both *in vitro* and *in vivo*, suggesting that the increase of the ratio of Bax/Bcl-2 might be the key factor of SW-induced apoptosis. These results provide further insight into SW-induced apoptosis and deepen the mechanisms of anticancer activity of SW, and can provide a rationale for developing SW to be a promising chemotherapeutic agent in future.

In summary, our results demonstrate that SW is an inducer of apoptosis in A549 cells. The SW-induced apoptosis is dependent on the mitochondria-mediated caspase activation and involvement of the regulation of Bcl-2 and Bax (Fig. 7). These data provided a clue to understand the mechanisms of SW-induced apoptosis. It is probable that we are far from unveiling the complete mechanisms underlying SW induction of the growth inhibition and apoptosis of tumor cells, and that other signaling components such as p53 might be involved. Work ongoing in our laboratory is addressing these issues.

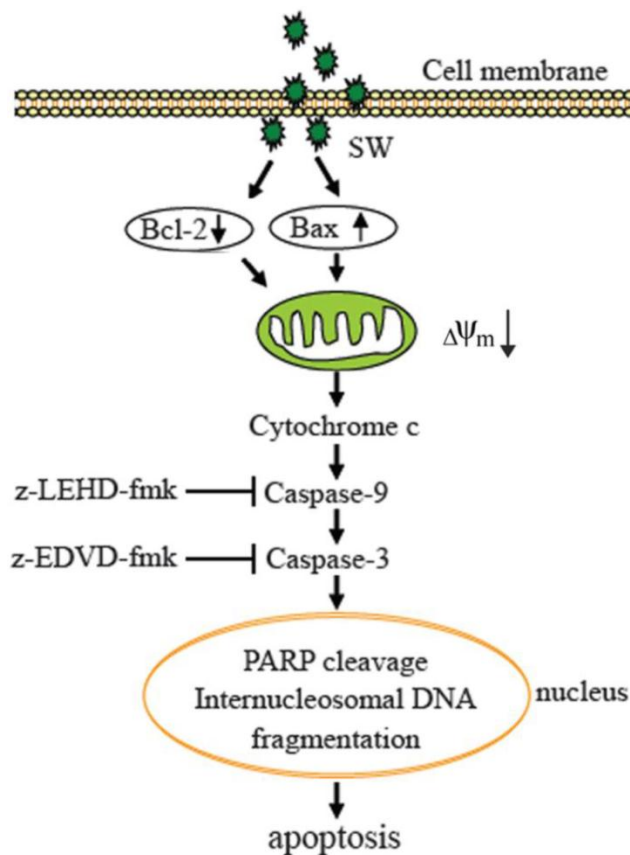


Figure 7. Proposed model of molecular mechanism of SW-induced apoptosis in A549 cells. SW treatment up-regulates Bax, down-regulates Bcl-2 expression, promotes Bax translocation to mitochondria, activates mitochondria-mediated apoptotic pathway, which in turn causes the release of cytochrome c, the activation of caspase-9 and caspase-3, and the cleavage of PARP and fragmentation of internucleosomal DNA, resulting in A549 cell apoptosis.

Acknowledgements

This work was supported by the National Natural Science Foundation of China (Grant No. 31072108), the Doctoral Program of Higher Education of China (Grant No. 20090204110016, 20110204110014) and the Fundamental Research Funds for the Central Universities (QN2011064). We are grateful to Yong Zhao and Kai Lei for their kind help in the animal experiments. The authors also thank Xin He for Flow cytometry assay, and Li Cao for help in statistical analysis.

Conflict of Interests

The authors have declared that no conflict of interest exists.

References

1. Colegate S, Dorling P, Huxtable C. A spectroscopic investigation of swainsonine: an α -mannosidase inhibitor isolated from *Swainsona canescens*. Aust J Chem. 1979; 32: 2257-64.
2. Molyneux R, James L. Loco intoxication: indolizidine alkaloids of spotted locoweed (*Astragalus lentiginosus*). Science. 1982; 216: 190-1.
3. Cao GR, Li SJ, Duan DX, et al. The toxic principle of Chinese locoweeds (*Oxytropis* and *Astragalus*): toxicity in goats. In: James LF, Keeler RF, Cheeke PR, Bailey EM, Hegarty MP, eds. Ames: Iowa State University Press. 1992: 117-21.
4. Tong D, Mu P, Dong Q, et al. Immunological evaluation of SW-HSA conjugate on goats. Colloids and Surfaces B: Biointerfaces. 2007; 58: 61-7.
5. Tong DW, Wang JY, Mu PH, et al. Analysis of several serum enzymes and blood urea nitrogen of swainsonine-HSA immunized goats. Anim Feed Sci Tech. 2008; 142: 74-88.
6. Dennis J, Laferte S, Yagel S, Breitman M. Asparagine-linked oligosaccharides associated with metastatic cancer. Cancer cells. 1989; 1: 87-92.
7. Dennis JW, Laferte S, Waghorne C, et al. Beta 1-6 branching of Asn-linked oligosaccharides is directly associated with metastasis. Science. 1987; 236: 582-5.
8. Dennis JW, Koch K, Yousefi S, VanderElst I. Growth inhibition of human melanoma tumor xenografts in athymic nude mice by swainsonine. Cancer Res. 1990; 50: 1867-72.
9. Sun JY, Zhu MZ, Wang SW, et al. Inhibition of the growth of human gastric carcinoma *in vivo* and *in vitro* by swainsonine. Phytomedicine. 2007; 14: 353-9.
10. Sun JY, Yang H, Miao S, et al. Suppressive effects of swainsonine on C6 glioma cell *in vitro* and *in vivo*. Phytomedicine. 2009; 16: 1070-4.
11. Dennis JW, Koch K, Beckner D. Inhibition of human HT29 colon carcinoma growth *in vitro* and *in vivo* by swainsonine and human interferon- α 2. J Natl Cancer I. 1989; 81: 1028-33.
12. Goss PE, Baptiste J, Fernandes B, et al. A phase I study of swainsonine in patients with advanced malignancies. Cancer Res. 1994; 54: 1450-7.
13. Goss PE, Reid CL, Bailey D, Dennis JW. Phase IB clinical trial of the oligosaccharide processing inhibitor swainsonine in patients with advanced malignancies. Clin Cancer Res. 1997; 3: 1077-86.
14. Klein JLD, Roberts J, George M, et al. Swainsonine protects both murine and human haematopoietic systems from chemotherapeutic toxicity. Brit J Cancer. 1999; 80: 87-95.
15. Oredipe OA, Furbert-Harris PM, Laniyan I, et al. Enhanced proliferation of functionally competent bone marrow cells in different strains of mice treated with swainsonine. Int Immunopharmacol. 2003; 3: 445-55.
16. Oredipe OA, White SL, Grzegorzewski K, et al. Protective effects of swainsonine on murine survival and bone marrow proliferation during cytotoxic chemotherapy. J Natl Cancer I. 1991; 83: 1149-56.
17. Hamaguchi J, Nakagawa H, Takahashi M, et al. Swainsonine reduces 5-fluorouracil tolerance in the multistage resistance of colorectal cancer cell lines. Mol Cancer. 2007; 6: 58.
18. Santos FM, Latorre AO, Hueza IM, et al. Increased antitumor efficacy by the combined administration of swainsonine and cisplatin *in vivo*. Phytomedicine. 2011; 18: 1096-1101.
19. Fadeel B, Orrenius S. Apoptosis: a basic biological phenomenon with wide-ranging implications in human disease. J Int Med. 2005; 258: 479-517.
20. Ghobrial IM, Witzig TE, Adjei AA. Targeting apoptosis pathways in cancer therapy. CA-Cancer J Clin. 2005; 55: 178-94.
21. Livak KJ, Schmittgen TD. Analysis of relative gene expression data using real-time quantitative PCR and the $2^{-\Delta\Delta Ct}$ method. Methods. 2001; 25: 402-8.
22. Li H, Zhu H, Xu C, Yuan J. Cleavage of BID by caspase 8 mediates the mitochondrial damage in the Fas pathway of apoptosis. Cell. 1998; 94: 491-501.
23. Li P, Nijhawan D, Budihardjo I, et al. Cytochrome c and dATP-dependent formation of Apaf-1/caspase-9 complex initiates an apoptotic protease cascade. Cell. 1997; 91: 479-89.
24. Sharpe JC, Arnoult D, Youle RJ. Control of mitochondrial permeability by Bcl-2 family members. BBA-Mol Cell Res. 2004; 1644: 107-13.
25. Yang WL, Addona T, Nair DG, et al. Apoptosis induced by cryo-injury in human colorectal cancer cells is associated with mitochondrial dysfunction. Int J Cancer. 2003; 103: 360-9.
26. Yagita M, Saksela E. Swainsonine, an inhibitor of glycoprotein processing, enhances cytotoxicity of large granular lymphocytes. Scand J Immunol. 1990; 31: 275-82.
27. Surh YJ. Cancer chemoprevention with dietary phytochemicals. Nat Rev Cancer. 2003; 3: 768-80.
28. Xu Y, Ge R, Du J, et al. Corosolic acid induces apoptosis through mitochondrial pathway and caspases activation in human cervix adenocarcinoma HeLa cells. Cancer Lett. 2009; 284: 229-37.
29. Cornil I, Kerbel RS, Dennis JW. Tumor cell surface beta 1-4-linked galactose binds to lectin(s) on microvascular endothelial cells and contributes to organ colonization. Journal Cell Bio. 1990; 111: 773-81.
30. Grzegorzewski K, Newton S, Akiyama S, et al. Induction of macrophage tumoricidal activity, major histocompatibility complex class II antigen (Iak) expression, and interleukin-1 production by swainsonine. Cancer Commun. 1989; 1: 373-9.
31. Humphries MJ, Matsumoto K, White SL, et al. Augmentation of murine natural killer cell activity by swainsonine, a new antimetastatic immunomodulator. Cancer Res. 1988; 48: 1410-5.
32. Kim RH, Coates JM, Bowles TL, et al. Arginine deiminase as a novel therapy for prostate cancer induces autophagy and caspase-independent apoptosis. Cancer Res. 2009; 69: 700-8.
33. Chu WF, Wu DM, Liu W, et al. Sulforaphane induces G2-M arrest and apoptosis in high metastasis cell line of salivary gland adenoid cystic carcinoma. Oral onco. 2009; 45: 998-1004.
34. Sun W, Xu W, Liu H, et al. γ -Tocotrienol induces mitochondria-mediated apoptosis in human gastric adenocarcinoma SGC-7901 cells. J Nutr Biochem. 2009; 20: 276-84.
35. Kroemer G, Reed JC. Mitochondrial control of cell death. Nat Med. 2000; 6: 513-9.
36. Huang YT, Huang DM, Chueh SC, et al. Alisol B acetate, a triterpene from *Alismatis rhizoma*, induces Bax nuclear translocation and apoptosis in human hormone-resistant prostate cancer PC-3 cells. Cancer Lett. 2006; 231: 270-8.